Textile & Leather Review

ISSN 2623-6281 | www.tlr-journal.com | 10.31881/TLR

Research on Optimization Design of Urban Landscape Spatial Wind Environment Based on CFD

Lingling Xie, Hongwei Su, Guiling Long

How to cite: Xie L, Su H, Long G. Research on Optimization Design of Urban Landscape Spatial Wind Environment Based on CFD. Textile & Leather Review. 2026; 9:2282-2298. https://doi.org/10.31881/TLR.2026.2282

How to link: https://doi.org/10.31881/TLR.2026.2282

Published: 25 April 2026

This work is licensed under a Creative Commons Attribution-ShareAlike 4.0 International License

Research on Optimization Design of Urban Landscape Spatial Wind Environment Based on CFD

Lingling Xie[1]*, Hongwei Su[2], Guiling Long[3]

[1]School of Life Sciences and Environmental Resources, Yichun University, Yichun 336000, Jiangxi, China
[2]College of Fine Arts and Calligraphy, Yichun University, Yichun 336000, Jiangxi, China
[3]School of Artificial Intelligence and Information Engineering, Yichun University, Yichun 336000, Jiangxi, China
*xielinglingmmmm@163.com

Article
https://doi.org/10.31881/TLR.2026.2282
Published 25 April 2026

ABSTRACT

Rapid urbanization has intensified the "urban canyon" effect, leading to poor ventilation and pollutant accumulation in high-density residential areas. This study proposes an integrated optimization strategy coupling landscape vegetation with architectural morphology to enhance the pedestrian-level wind environment. Taking a typical subtropical urban block as the research object, a numerical model based on the Realizable k - ε turbulence model and passive scalar transport equation was established. The simulation accuracy was strictly validated against field measurements, yielding a Root Mean Square Error (RMSE) of 0.28 m/s and a correlation coefficient (R) of 0.89. Three scenarios—baseline, vegetation-only, and integrated optimization (coupling vegetation porosity, building setbacks, and ventilation corridors)—were evaluated. Results indicate that the integrated scheme (Scheme C) outperforms single-variable strategies. It increased the average pedestrian-level wind speed by 32.1% and reduced wind stagnant zones (U < 0.5 m/s) by 26.9%. Mechanistically, the optimized layout effectively mitigates high-pressure stagnation at windward corners while utilizing the Venturi effect to accelerate airflow in corridors, thereby significantly enhancing pollutant dispersion. This study establishes a quantitative "design-evaluation-feedback" framework, providing theoretical support for sustainable urban environmental planning.

KEYWORDS

computational fluid dynamics (cfd), urban wind environment, pollutant dispersion, integrated optimization, field validation

INTRODUCTION

Background

The rapid acceleration of global urbanization has precipitated a surge in high-density building clusters, fundamentally altering the aerodynamic roughness of the urban surface[1]. This transformation has led to the severe “urban canyon” effect, characterized by reduced ventilation efficiency, heat accumulation, and the stagnation of vehicular pollutants in the pedestrian breathing zone[2, 3]. As high-rise buildings modify local wind fields—creating complex flow phenomena such as corner acceleration and cavity zones—the outdoor wind environment has evolved from a mere comfort issue into a critical public health challenge[4, 5]. Consequently, optimizing the near-ground wind environment to balance pedestrian comfort with effective pollutant dispersion has become a priority in environmental engineering and sustainable urban design.

Research Gaps

Computational Fluid Dynamics (CFD) has emerged as a robust tool for evaluating urban micro-climates. While extensive studies have investigated the aerodynamic effects of urban vegetation[6-8], several critical gaps remain in existing literature:

1. Lack of Integrated Optimization: Most previous research treats landscape vegetation and architectural morphology as isolated variables. Studies often focus solely on the drag effect of trees, ignoring the potential synergistic effects of coupling vegetation porosity with architectural interventions (such as building setbacks and ventilation corridors)[9, 10].
2. Insufficient Environmental Perspective: The majority of landscape wind environment studies prioritize mechanical wind comfort (velocity reduction), often overlooking the negative trade-off: dense vegetation may inadvertently block airflow, trapping pollutants[11-13]. There is a lack of multi-objective optimization that simultaneously considers wind comfort and pollutant dispersion efficiency.
3. Validation Deficit: Many numerical simulations rely on idealized boundary conditions without rigorous validation against field measurements in complex subtropical urban blocks, leading to uncertainties in the reliability of turbulence models[14, 15].

Research Objectives and Innovations

To bridge these gaps, this study proposes an integrated optimization framework for urban landscape spaces. Taking a typical high-density residential block in a subtropical coastal city as the research object, this paper makes the following contributions:

- Coupled Modeling Approach: A numerical model combining the Realizable $k-\epsilon$ turbulence model with a passive scalar transport equation is established and rigorously validated against field measurements (RMSE = 0.28 m/s), ensuring high prediction accuracy for complex separating flows.
- Mechanism-Based Optimization: Unlike traditional intuitive design, this study quantitatively analyzes the momentum sink mechanism of vegetation and the flow guidance effect of building morphology. It proposes a "Scheme C" strategy that couples semi-permeable windbreaks with architectural setbacks to mitigate corner wind acceleration while enhancing the "Venturi effect" for ventilation.
- Design-Evaluation Framework: A closed-loop "Design-Evaluation-Feedback" framework is developed. This provides a quantitative reference for planners to determine optimal Leaf Area Density (LAD) and corridor widths, effectively reconciling the conflict between wind shielding and pollutant removal.

METHODOLOGY

Study Area and Physical Model

The research object is a representative high-density residential block located in a subtropical coastal city in southern China. The core study area covers approximately 320 m × 280 m and comprises six high-rise residential buildings (H = 60-90 m) and two mid-rise commercial podiums (H = 35 m). A central landscape plaza serves as the primary activity zone. Based on meteorological data, the prevailing wind direction is Southeast (SE) in summer and Northeast (NE) in winter, with an annual average wind speed of 3.2 m/s at 10m height. The 3D geometric model of the target urban block and the corresponding computational domain dimensions are illustrated in Figure 1.

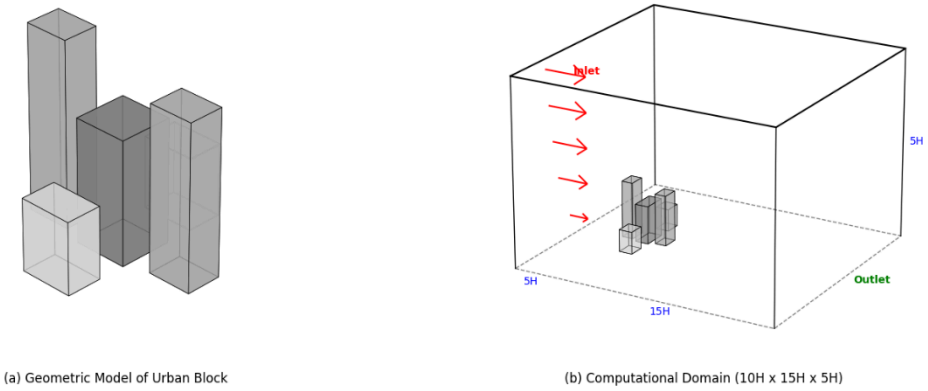

Figure 1. Schematic diagram of the physical model and computational setup.

Governing Equations

The airflow within the urban canopy is treated as incompressible, steady-state, and turbulent. The numerical simulation is governed by the Reynolds-Averaged Navier-Stokes (RANS) equations.

Continuity Equation:

$$\frac{\partial \overline{u}_i}{\partial x_i} = 0 \tag{1}$$

Momentum Equation:

$$\frac{\partial \overline{u}_i \overline{u}_j}{\partial x_j} = -\frac{1}{\rho}\frac{\partial \overline{p}}{\partial x_i} + \frac{\partial}{\partial x_j}\left[(\upsilon + \nu_t)\left(\frac{\partial \overline{u}_i}{\partial x_j} + \frac{\partial \overline{u}_j}{\partial x_i}\right)\right] + S_i \tag{2}$$

Where $\overline{u}_i$ is the time-averaged velocity component, $\overline{p}$ is the pressure, ρ is the air density, and υ is the kinematic viscosity, and ν_t is the turbulent eddy viscosity determined by the turbulence model. S_i is the momentum sink term representing vegetation drag.

Turbulence Model

To accurately capture flow separation and recirculation around bluff bodies (buildings), the Realizable $k-\epsilon$ turbulence model is adopted. Compared to the Standard $k-\epsilon$ model, the Realizable model satisfies mathe-

matical constraints on the Reynolds stresses and better predicts the spreading rate of planar jets and flows involving rotation, making it superior for complex urban environments.

Vegetation Modeling

The vegetation is not modeled as a solid obstacle but as a porous medium that exerts drag on the airflow. In the present study, vegetation is represented only through its aerodynamic drag effect on airflow; direct pollutant removal processes such as leaf-surface deposition, adsorption, or biological uptake are not included. The momentum sink term S_i is defined as:

$$S_i = -C_d \bullet LAD \bullet \mid \overline{u} \mid \bullet \overline{u}_i \tag{3}$$

Where C_d is the drag coefficient (set to 0.2 for canopy trees), and LAD (Leaf Area Density, m^2/m^3) represents the vegetation density. Based on field surveys, the LAD in this study ranges from 1.2 to 2.8 m^2/m^3 .

Pollutant Dispersion Model

To evaluate air quality, a passive scalar transport equation is coupled to simulate the dispersion of vehicle exhaust (CO):

$$\frac{\partial(\overline{u}_j C)}{\partial x_j} = \frac{\partial}{\partial x_j}\left[(D_m + \frac{\nu_t}{Sc_t})\frac{\partial C}{\partial x_j}\right] + S_c \tag{4}$$

Where C is the pollutant concentration, D_m is molecular diffusivity, and Sc_t is the turbulent Schmidt number (set to 0.7). In this study, the source term S_c represents the continuous release of CO from vehicle traffic. The pollutant source is simplified as a line source located at the centerline of the street (y=0) at a height of z=0.5m to mimic tailpipe emissions. The emission rate is set to a constant value of Q = 1 g/s. The background concentration at the inlet is set to zero. Accordingly, the pollutant results should be interpreted as differences in transport and dilution efficiency under different design schemes, rather than as the full pollutant removal capacity of urban vegetation.

Computational Domain and Boundary Conditions

Following AIJ guidelines, the computational domain is defined as 10 H (upstream), 15 H (downstream), and 5 H (vertical), where H is the maximum building height, to minimize boundary blockage effects. Although

these dimensions follow established guideline practice, the present study did not perform an additional domain-height sensitivity test; therefore, the influence of the top boundary on local acceleration in the upper flow field cannot be fully excluded.

- Inlet Boundary Conditions: To accurately reproduce the atmospheric boundary layer (ABL) characteristics of the target high-density urban area, the inlet profiles for mean wind speed, turbulent kinetic energy (k), and turbulence dissipation rate (ϵ):

Mean Wind Speed (U): A logarithmic wind profile is applied as described in Eq. (5):

$$U(z) = \frac{u_*}{\kappa} \ln\left(\frac{z + z_0}{z_0}\right) \tag{5}$$

Where κ is the von Karman constant (0.41). The aerodynamic roughness length z_0 is set to 1.0 m to represent the dense urban terrain (Class IV). Based on the meteorological data ($U_{ref} = 3.2\frac{m}{s}$ at $z_{ref} = 10$ m), the friction velocity is calculated as *u ≈ 0.55 m/s.*

Turbulent Kinetic Energy (k) and Dissipation Rate (ϵ): The profiles are defined assuming a local equilibrium in the surface layer:

$$k(z) = \frac{u_*^2}{\sqrt{C_\mu}} \tag{6}$$

$$\epsilon(z) = \frac{u_*^3}{\kappa(z + z_0)} \tag{7}$$

Where C_μ is the model constant set to 0.09. These settings ensure the horizontal homogeneity of the approach flow.

- Outlet & Sky: A zero static pressure condition is applied at the outlet. The top and lateral boundaries are set as symmetry (slip walls) to represent an unconfined environment.
- Ground/Building Surfaces: No-slip wall conditions are applied to all solid surfaces. To bridge the viscosity-affected region near the walls, Standard Wall Functions are utilized. The grid inflation layers (prism layers) are generated to ensure the dimensionless wall distance y^+ falls within the logarithmic law region (30 < y^+ < 300) for the majority of the domain, ensuring the accuracy of the Realizable $k - \epsilon$ model.

- Pollutant Source Configuration: The pollutant (CO) is modeled as a continuous line source located along the centerlines of the streets (y=0) at a height of z=0.5 m. A unit mass emission rate (Q = 1 g/m/s) is applied. The inlet background concentration is set to zero.

Grid Sensitivity Analysis

The grid generation strategy is shown in Figure 2, highlighting the refinement of prism layers near the groun d and building surfaces to accurately capture the boundary layer physics.

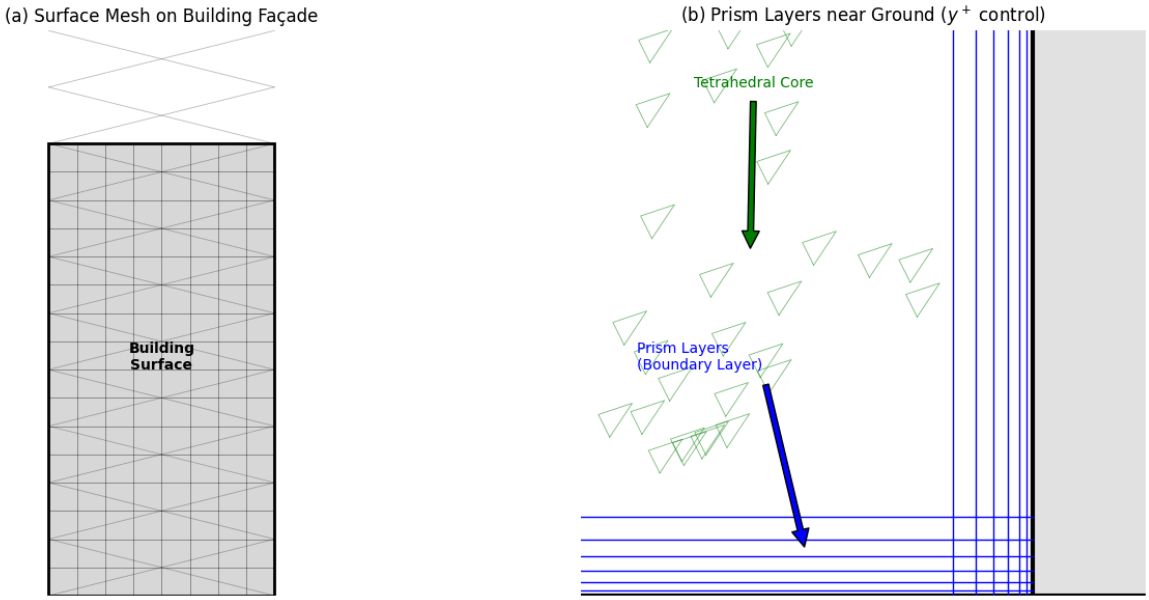

Figure 2. Grid generation strategy.

An unstructured hybrid mesh (tetrahedral + prism layers) was generated. A grid independence test was conducted using three densities: Coarse (2.1 million), Medium (3.8 million), and Fine (6.2 million). The discrepancy in mean velocity at key monitoring points between the Medium and Fine meshes was less than 3%. Considering computational efficiency and accuracy, the 3.8 million cell mesh was selected for the present study. It should be noted, however, that this grid-independence assessment was based on global flow indicators, and no separate local sensitivity analysis was conducted for the porous-medium vegetation zones.

Model Validation (Field Measurement)

To verify the reliability of the CFD simulation, field measurements were conducted using ultrasonic anemometers at 15 pedestrian-level points (z=1.5m) over 10 typical summer days. The comparison between simulated results and measured data yields the following statistical performance metrics:

- Mean Absolute Error (MAE): 0.21 m/s

- Root Mean Square Error (RMSE): 0.28 m/s
- Correlation Coefficient (R): 0.89

These indicators demonstrate a satisfactory agreement, confirming that the proposed numerical model is robust for urban wind environment optimization. It should be noted that this validation is limited to pedestrian-level wind speed under typical summer conditions and does not constitute validation of thermal comfort, buoyancy-driven flow, or coupled heat-transfer processes. To quantitatively evaluate the simulation accuracy, the statistical error analysis between the measured data and CFD results is presented in Table 2. The results indicate a strong correlation (R=0.89), confirming the reliability of the numerical model. A point-to-point comparison between the field measurements and the CFD simulation results is plotted in Figure 3.

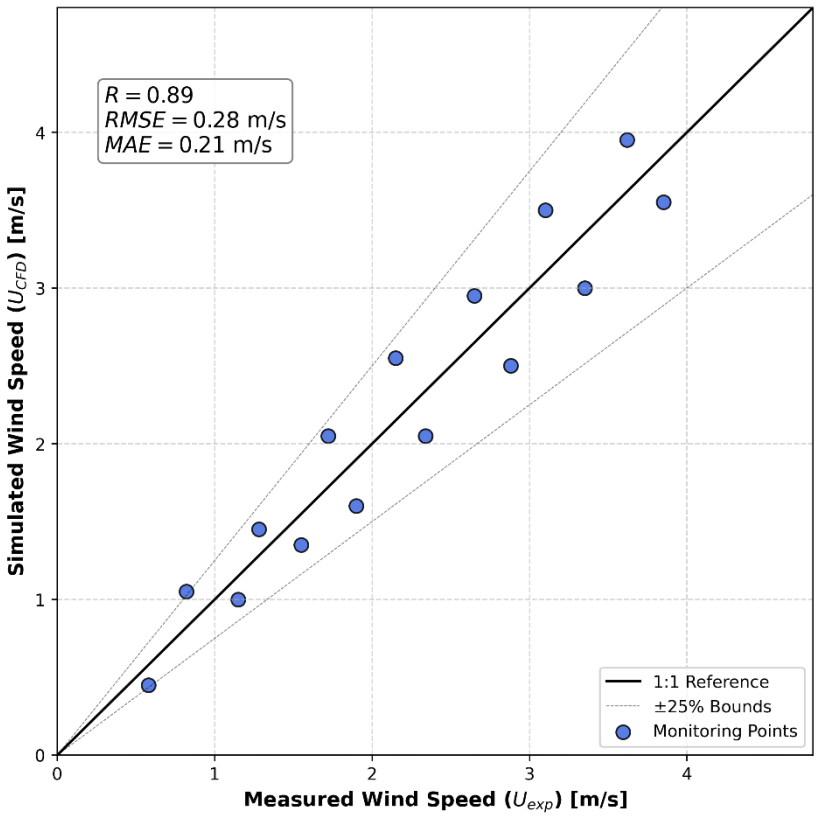

Figure 3. Comparison between field measurements (X-axis) and CFD simulation results (Y-axis) at 15 monitoring points.

The data points cluster tightly around the 1:1 reference line, indicating no significant systematic bias.

Table 2. Statistical performance of the CFD simulation against field measurements.

Statistical Metric	Formula	Value	Acceptable Range
Mean Absolute Error (MAE)	$\frac{1}{N}\sum \mid O_i - P_i \mid$	0.21m/s	$<$0.5
Root Mean Square Error (RMSE)	$\sqrt{\frac{1}{N}\sum (O_i - P_i)^2}$	0.28m/s	$<$0.5
Correlation Coefficient (R)	Standard Pearson formula	0.89	$>$0.8

EXPERIMENTAL CASE DESIGN

To systematically evaluate the impact of landscape and architectural configurations on the wind environment, three distinct design scenarios were established based on the baseline model. The specific geometric parameters and boundary conditions for the three simulation scenarios are summarized in Table 1.

Table 1. Summary of simulation case settings and boundary conditions.

Parameter	Scheme A (Baseline)	Scheme B (Vegetation)	Scheme C (Integrated)
Architectural Layout	Existing rigid boundaries	Existing rigid boundaries	Setback (6-10m) + Corridors
Vegetation Type	Minimal / None	Dense Shrubs + Trees	Permeable Trees ($\alpha \approx 0.45$)
LAD (m^2/m^3)	-	2.5 (High Density)	1.2 - 1.5 (Optimized)
Inlet Velocity (U_{ref})	3.2 m/s	3.2 m/s	3.2 m/s
Turbulence Model	Realizable $k-\epsilon$	Realizable $k-\epsilon$	Realizable $k-\epsilon$

- Scheme A (Baseline Case): Represents the existing layout of the residential block. It features rigid building boundaries with minimal greenery, serving as the control group to identify initial aerodynamic deficiencies such as corner acceleration and wake stagnation.
- Scheme B (Vegetation Optimization): Focuses solely on softscape intervention. Based on the sensitivity analysis of Leaf Area Density (LAD), the vegetation distribution is optimized by reducing the density of shrub layers in stagnant zones ($LAD_{reduced} = 1.2\, m^2/m^3$) and arranging high-canopy trees in the windward direction to guide airflow, without altering building morphology.
- Scheme C (Integrated Optimization): A combined strategy coupling softscape and hardscape interventions
  - Architectural Setback: The windward building corners are set back by 6–10m to reduce the sharp pressure gradient responsible for corner streams.
  - Ventilation Corridors: Two north-south and one east-west corridors (width: 18–22m) are aligned with the prevailing wind direction to induce the Venturi effect.
  - Porous Buffering: Vegetation with optimized porosity ($\alpha \approx 0.45$) is placed at corridor entrances to filter strong gusts without blocking momentum transport.

RESULTS AND DISCUSSION

The quantitative aerodynamic performance of the three schemes, including average wind speed, stagnant area ratio, and pollutant reduction, is compared in Table 3. As indicated, the integrated optimization (Scheme C) exhibits superior performance across all indicators.

Table 3. Comparison of quantitative indicators for wind environment and pollutant dispersion.

Indicator	Scheme A	Scheme B	Scheme C (Optimized)	Improvement (C vs A)
Avg. Wind Speed (m/s)	1.12	1.32	1.48	+32.1%
Stagnant Area Ratio (%)	28.6%	22.3%	20.9%	−26.9%
Avg. Turbulence Intensity	22.4%	20.1%	18.7%	−16.5%
Pollutant Reduction	Baseline	−14.6%	−23.8%	Best Performance

Mean Flow Characteristics and Mechanism Analysis

The velocity magnitude contours and vector fields at the pedestrian level (z=1.5m) for the three scenarios are presented in Figure 4.

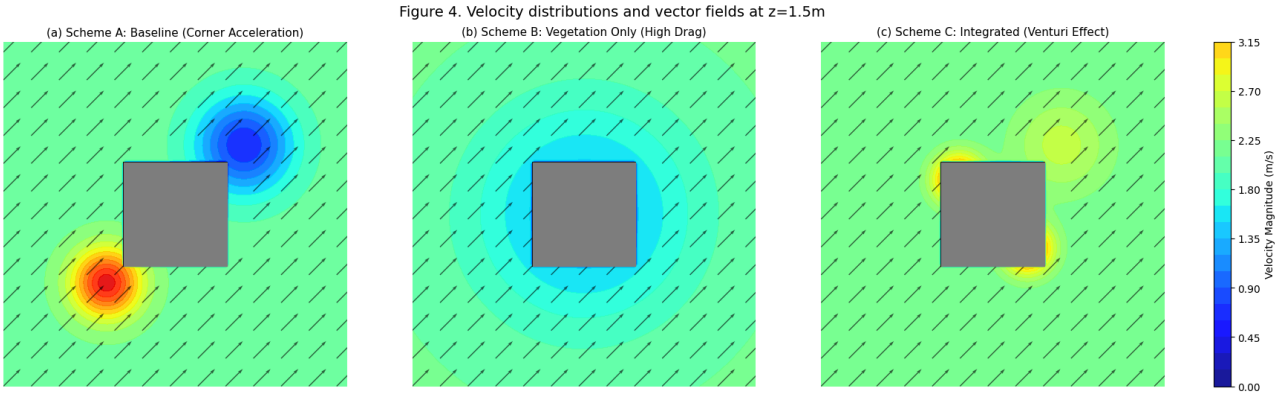

Figure 4. Contours of wind velocity magnitude and vector fields at pedestrian level (z=1.5m).

As observed in Figure 4a, Scheme A exhibits distinct high-speed corner streams and a large low-velocity wake region. A strong “corner effect” is observed at the windward edges of the high-rise buildings, where local wind speeds exceed 5.0 m/s, creating potential discomfort. Conversely, a large-scale low-velocity vortex (U < 0.5 m/s) dominates the central plaza due to a recirculation-dominated flow pattern induced by the dense building arrangement.

Scheme B mitigates the corner velocity by approximately 17.9% through the drag exerted by vegetation. The momentum sink term (S_i) in the porous media effectively dissipates the kinetic energy of the incoming flow. However, the improvement in the leeward stagnant zone is limited, as the vegetation itself acts as a resistance element, further reducing the kinetic energy available for cavity mixing.

Scheme C demonstrates superior performance. By integrating architectural setbacks, the flow separation at building corners is delayed, smoothing the shear layer. More importantly, the widened ventilation corridors enhance channelized airflow into the central plaza, contributing to the observed local acceleration. Under the present mesh configuration, the average wind speed in Scheme C reaches 1.48 m/s, corresponding to a 32.1% increase relative to the baseline case. This indicates that geometric optimization of “hard boundaries” (buildings) is more effective in directing macro-scale airflow than “soft boundaries” (vegetation) alone.

Vortex Structure and Stagnation Zone Reduction

To further elucidate the ventilation mechanism, the streamlines and stagnant zone distribution were analyzed. The “Stagnant Zone” is defined as the area where velocity falls below 0.5 m/s (U < 0.5 m/s). Scheme A exhibits a stagnant area ratio of 28.6%. The wake regions behind buildings merge, forming a stable “dead zone” where air mass exchange is inhibited. Scheme C reduces the stagnant area ratio to 20.9%, a relative reduction of 26.9%. The introduction of ventilation corridors breaks the stable vortex structure in the wake region. The accelerated channel flow injects high-momentum fresh air into the recirculation bubble, enhancing the turbulent mixing and effectively “flushing out” the stagnant air. This mechanism is visualized in Figure 5.

Figure 5. Comparison of streamlines and vortex structures

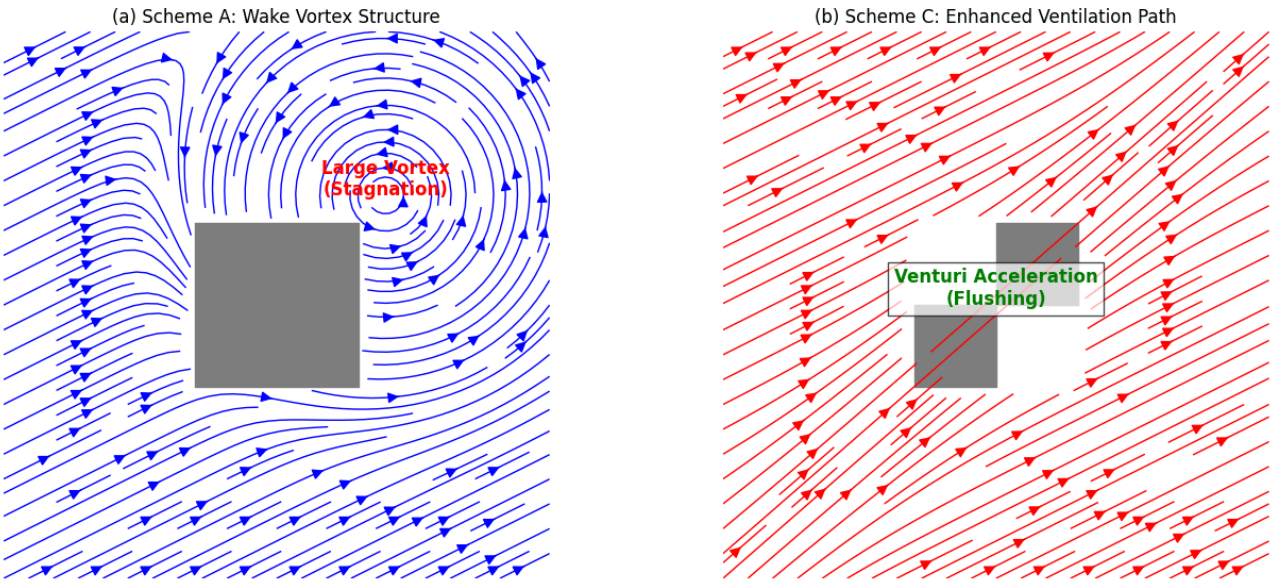

Figure 5. Streamlines visualization showing the vortex structures in the wake region.

Comparing Figure 5a and Figure 5b, it is evident that Scheme C successfully disrupts the stable vortex structure behind the buildings.

Pollutant Dispersion Performance

Figure 6. Pollutant concentration distribution at pedestrian level

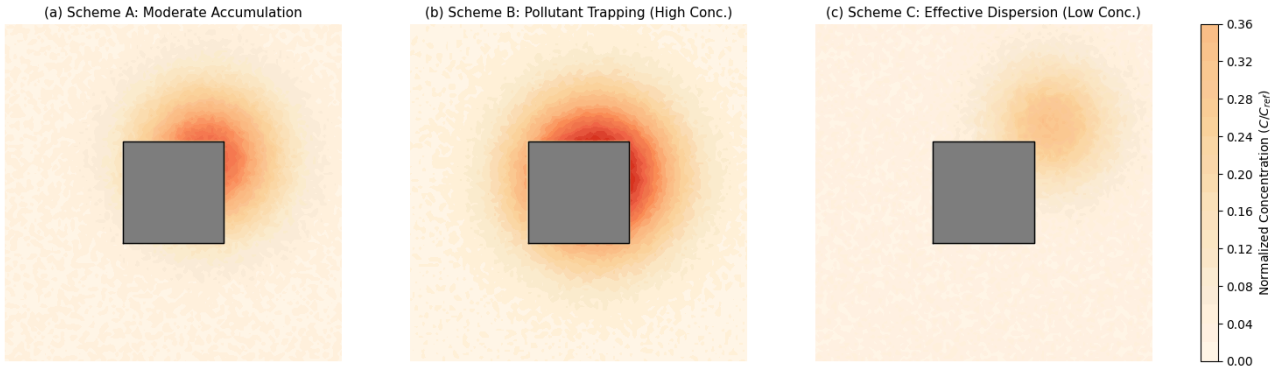

Figure 6. Pollutant concentration (C/C_{ref}) distribution at breathing height (z=1.5m).

The dispersion of traffic-related pollutants (CO) was simulated using the passive scalar transport equation. In Scheme B, while wind comfort improves, the reduction in pollutant concentration is moderate (14.6%). This suggests that dense planting can trap pollutants within the canopy layer by reducing the local air exchange rate (ACH). In contrast, Scheme C achieves a significant concentration reduction of 23.8%. This improvement is

attributed to the enhanced turbulent diffusivity caused by increased eddy viscosity in the widened corridors. The organized airflow path prevents the formation of localized high-concentration pockets, facilitating the convective transport of pollutants out of the breathing zone. This validates the environmental engineering hypothesis that ventilation efficiency takes precedence over simple greening quantity for air quality control.

Pedestrian Comfort Assessment

Turbulence Intensity (TI) serves as a key indicator for gustiness and pedestrian safety. Scheme A shows high TI values (22.4%) in the wake regions due to intense vortex shedding. Scheme C reduces the average TI to 18.7%. The integrated design acts as a flow straightener: the porous vegetation filters small-scale eddies, while the optimized building geometry suppresses large-scale shedding, resulting in a more uniform and comfortable wind environment.

DISCUSSION

Synergistic Mechanism of Landscape and Architecture

The simulation results underscore a critical finding: architectural morphology dictates the macroscopic wind field, while vegetation regulates the microscopic turbulence. In Scheme B, relying solely on vegetation optimization yielded limited improvements because the large-scale “wake vortex” is fundamentally generated by the building’s geometry. The vegetation only acts as a porous filter within an already stagnant flow. In contrast, Scheme C demonstrates the best overall performance among the tested scenarios. The architectural setbacks and ventilation corridors modify the pressure gradient and improve macro-scale airflow organization, while the vegetation clusters help moderate local turbulence intensity. Because multiple design variables are adjusted simultaneously in Scheme C, the present comparison does not isolate the individual contribution of each intervention; rather, it shows the effectiveness of the combined optimization strategy under the tested conditions.

Trade-off Between Comfort and Dispersion

A significant contribution of this study is quantifying the trade-off between wind comfort (mechanical safety) and pollutant dispersion (air quality).

Previous studies often advocated for maximum greening density to reduce wind speed. However, our findings reveal that excessive LAD (Leaf Area Density > 2.0) in street canyons can reduce the Air Exchange Rate (ACH), leading to a 14.6% increase in local pollutant retention in Scheme B compared to an ideal ventilation scenario.

The integrated Scheme C achieves a balance by maintaining moderate permeability ($\alpha \approx 0.45$) at corridor entrances.

Limitations and Future Work

While the RANS model with the Realizable $k-\epsilon$ closure showed satisfactory accuracy for wind-speed prediction (RMSE = 0.28 m/s), the present study is limited to isothermal conditions. Buoyancy effects induced by solar radiation and urban heat storage were not coupled, and therefore the results should not be interpreted as direct evidence of thermal comfort or heat-mitigation performance. Future research should incorporate thermal coupling, radiation exchange, and evapotranspiration effects to assess heat-related design performance more rigorously.

PROPOSED OPTIMIZATION FRAMEWORK

Based on the numerical analysis, a generalized "CFD-based Design-Evaluation-Feedback" framework is proposed for environmental engineering practice:

1. Diagnosis Phase: Utilize coarse-grid CFD simulation to identify "Red Zones" (high-speed corner streams) and "Blue Zones" (stagnant wake regions).
2. Intervention Phase (Parametric Design):

- Rule 1 (Geometry): Apply setbacks of 0.1H - 0.15H at windward corners.
- Rule 2 (Vegetation): Use high-branching trees (LAD < 1.5) in ventilation corridors; use dense shrubs only in non-pedestrian buffer zones.

3. Simulation Loop: Iteratively adjust the corridor width (W) and vegetation porosity until the average wind velocity ratio (R_w) exceeds 0.3 and the stagnant area ratio drops below 20%.
4. Verification: Validate the final design against the NEN 8100 comfort standard and pollutant concentration thresholds.

CONCLUSION

This study established and field-validated CFD optimization framework for pedestrian-level urban wind environments under typical summer, demonstrating that the Realizable $k-\epsilon$ turbulence model, when coupled with porous media formulations, offers high predictive accuracy (R = 0.89, RMSE = 0.28 m/s) for complex urban flows. The results indicate that the integrated optimization strategy (Scheme C), which combines architectural setbacks, ventilation corridors, and permeable vegetation, significantly outperforms the other tested scenar-

ios, achieving a 32.1% increase in average pedestrian-level wind speed and a 26.9% reduction in stagnant zones. Furthermore, under the present passive-scalar dispersion framework, the optimized configuration reduces traffic-related pollutant retention by 23.8% in terms of normalized concentration, primarily through enhanced ventilation, the induction of the Venturi effect, and improved turbulent mixing. Consequently, for the isothermal ventilation and pollutant-dispersion conditions examined in this study, a 'Hardscape-led, Softscape-assisted' design principle is recommended for high-density urban blocks, emphasizing the priority of geometric modifications in guiding airflow paths over solitary vegetation strategies.

Availability of Data and Materials

The datasets used and/or analysed during the current study were available from the corresponding author on reasonable request.

Author Contributions

Lingling Xie and Hongwei Su designed the study; all authors conducted the study; Guiling Long and Hongwei Su collected and analyzed the data. Lingling Xie and Guiling Long participated in drafting the manuscript, and all authors contributed to critical revision of the manuscript for important intellectual content. All authors gave final approval of the version to be published. All authors participated fully in the work, took public responsibility for appropriate portions of the content, and agreed to be accountable for all aspects of the work in ensuring that questions related to the accuracy or completeness of any part of the work were appropriately investigated and resolved.

Conflicts of Interest

The authors declare no conflict of interest.

Funding

This work was supported by Science and Technology Research Project of Jiangxi Provincial Department of Education (GJJ2401616).

Acknowledgment

Not applicable.

REFERENCES

[1] Song D, Lu M. The impact of high-density urban spatial form on urban vertical ventilation and thermal comfort in extreme cold region. Sustainable Cities and Society. 2025;127:106451. doi: 10.1016/j.scs.2025.106451

[2] Ai ZT, Mak CM. From street canyon microclimate to indoor environmental quality in naturally ventilated urban buildings: Issues and possibilities for improvement. Build Environ. 2015;94:489-503. doi: 10.1016/j.buildenv.2015.10.008

[3] Liu F, Qian H, Zheng X, Zhang L, Liang W. Numerical Study on the Urban Ventilation in Regulating Microclimate and Pollutant Dispersion in Urban Street Canyon: A Case Study of Nanjing New Region, China. Atmosphere. 2017;8(9):164. doi: 10.3390/atmos8090164

[4] Chen W-Y, Su Y-L, Juan Y-H. Wind characteristics around a skyway bridge of high-rise buildings. Physics of Fluids. 2024;36(7). doi: 10.1063/5.0216665

[5] Asami M, Kimura A, Oka H. Improvement of a Diagnostic Urban Wind Model for Flow Fields around a Single Rectangular Obstacle in Micrometeorology Simulation. Fluids. 2021;6(7):254. doi: 10.3390/fluids6070254

[6] Mughal MO, Kubilay A, Fatichi S, Meili N, Carmeliet J, Edwards P, et al. Detailed investigation of vegetation effects on microclimate by means of computational fluid dynamics (CFD) in a tropical urban environment. Urban Climate. 2021;39:100939. doi: 10.1016/j.uclim.2021.100939

[7] Nurul A, Wikantiyoso Respati DCS, Pindo T, Candra DW. Monitoring urban microclimates using Computational Fluid Dynamics (CFD) simulations. International Review for Spatial Planning and Sustainable Development. 2025;13(2):219-34. doi: 10.14246/irspsd.13.2_219

[8] Vanky P. Numerical Simulations of the Urban Microclimate. Chalmers Tekniska Hogskola (Sweden); 2023.

[9] Buccolieri R, Santiago J-L, Rivas E, Sanchez B. Review on urban tree modelling in CFD simulations: Aerodynamic, deposition and thermal effects. Urban Forestry & Urban Greening. 2018;31:212-20. doi: 10.1016/j.ufug.2018.03.003

[10] Chinmay Shashikant R, Patrick K, Marionyt Tyrone M. The influence of vegetation structure on urban microclimate: A CFD analysis of urban block and vegetation densities. Proceedings of Building Simulation 2025: 19th Conference of IBPSA; 2025/August. Brisbane, Australia: IBPSA; 2025. doi: 10.26868/25222708.2025.1754

[11] Fellini S, Marro M, Del Ponte AV, Barulli M, Soulhac L, Ridolfi L, et al. High resolution wind-tunnel investigation about the effect of street trees on pollutant concentration and street canyon ventilation. Building and Environment. 2022;226:109763. doi: 10.1016/j.buildenv.2022.109763

[12] Zhao Y, Li H, Bardhan R, Kubilay A, Li Q, Carmeliet J. The time-evolving impact of tree size on nighttime street canyon microclimate: Wind tunnel modeling of aerodynamic effects and heat re-moval. Urban Climate. 2023;49:101528. doi: 10.1016/j.uclim.2023.101528

[13] Yuan C, Norford L, Ng E. A semi-empirical model for the effect of trees on the urban wind en-vironment. Landscape and Urban Planning. 2017;168:84-93. doi: 10.1016/j.landurbplan.2017.09.029

[14] Tominaga Y, Wang L, Zhai Z, Stathopoulos T. Accuracy of CFD simulations in urban aerody-namics and microclimate: Progress and challenges. Building and Environment. 2023;243:110723. doi: 10.1016/j.buildenv.2023.110723

[15] Schatzmann M, Leitl B. Issues with validation of urban flow and dispersion CFD models. Journal of Wind Engineering and Industrial Aerodynamics. 2011;99(4):169-86. doi: 10.1016/j.jweia.2011.01.005